ELSEVIER

Chemical Geology 182 (2002) 227–235

CHEMICAL GEOLOGY
INCLUDING
ISOTOPE GEOSCIENCE

www.elsevier.com/locate/chemgeo

Mantle melting beneath Gakkel Ridge (Arctic Ocean): abyssal peridotite spinel compositions

Eric Hellebrand [a,*], Jonathan E. Snow [a], Richard Mühe [b]

[a] *Max-Planck-Institut für Chemie, Abt. Geochemie, Postfach 3060, D-55020 Mainz, Germany*
[b] *Institut für Geowissenschaften, Universität Kiel, Olshausenstrasse 40, D-24118 Kiel, Germany*

Received 10 July 2000; accepted 26 March 2001

Abstract

The ultraslow spreading Gakkel Ridge represents one of the most extreme spreading environments on the Earth. Full spreading rates there of 0.6–1.3 cm/year and $Na_{8.0}$ in basalts of 3.3 imply an extremely low degree of mantle partial melting. For this reason, the complementary degree of melting registered by abyssal peridotite melting residues is highly interesting. In a single sample of serpentinized peridotite from Gakkel Ridge, we found spinels which, though locally altered, have otherwise unzoned and thus primary compositions in the cores of the grains. These reflect a somewhat higher degree of melting of the uppermost oceanic mantle than indicated by basalt compositions. Cr/(Cr + Al) ratios of these grains lie between 0.23 and 0.24, which is significantly higher than spinels from peridotites collected along the faster spreading Mid-Atlantic and Southwest Indian Ridges. Crustal thickness at Gakkel Ridge can be calculated from the peridotite spinel compositions, and is thicker than the crustal thickness of less than 4 km estimated from gravity data, or predicted from global correlations between spreading rate and seismically determined crustal thickness. The reason for this unexpected result may be local heterogeneity due to enhanced melt focussing at an ultraslow spreading ridge.

Keywords: Abyssal peridotite; Spinel; Melting; Arctic; Gakkel Ridge

1. Introduction

Gakkel Ridge extends for 1800 km in the Arctic Ocean from the north coast of Greenland to the north coast of Siberia (Fig. 1). It is the world's slowest-spreading mid-ocean ridge, with full spreading rates ranging from 1.3 cm/year at the European end of the ridge to 0.6 cm/year at the Siberian end in the Laptev Sea. The fastest part of Gakkel Ridge is thus slower than the slowest part of the next most well-studied ultraslow-spreading ridge, the Southwest Indian Ridge (SWIR). Gakkel Ridge is characterized by an extremely deep rift valley, with axial depths between 4600 and 5100 m (Coakley and Cochran, 1998). Major transform offsets are absent, and the spreading is completely orthogonal.

Except for a few basaltic glass shards and altered basalt fragments from two sediment cores (Mühe et

* Corresponding author. Tel.: +49-6131-305-220; fax: +49-6131-371-051.
E-mail address: ehelle@mpch-mainz.mpg.de (E. Hellebrand).

0009-2541/02/$ - see front matter
PII: S0009-2541(01)00291-1

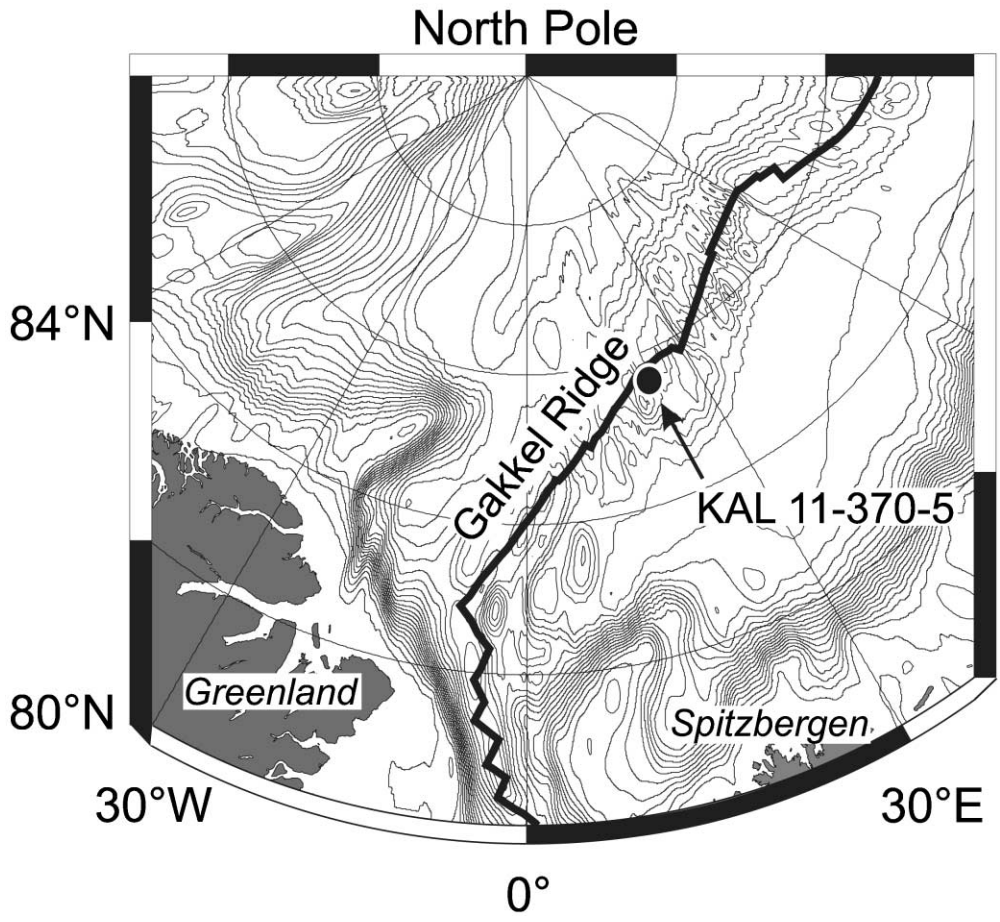

Fig. 1. Bathymetric map of the Arctic Ocean, showing the ultraslow spreading Gakkel Ridge, and the sampling location of box core ARK IV/3: KAL 11-370-5.

al., 1991, 1993, 1997), little is known about the chemical composition of Gakkel Ridge crust and mantle. The basalts have extremely high $Na_{8.0}$ and chondrite-normalized Sm/Yb ratios of 1.4–1.5 and appear to be the products of very low degrees of mantle melting, confirming its end member position in the global correlation between basalt chemistry and extent of mantle melting beneath ocean ridges (Klein and Langmuir, 1987; Langmuir et al., 1992). Further, gravity studies estimate a crustal thickness between 1 and 4 km for the western part of Gakkel Ridge (Coakley and Cochran, 1998), much lower than the canonical 6–7-km crust observed beneath the remainder of the Earth's oceans. This is in accordance with simple thermal models predicting a sharp drop-off in crustal thickness at spreading rates under 2–3 cm/year (Reid and Jackson, 1981).

Spinel composition is a useful tracer of melting in residual peridotites (Dick and Bullen, 1984; Hellebrand et al., 2001). The relative degree of melting estimated from abyssal peridotite spinel compositions is thought to be correlated with spreading rate (Niu and Hekinian, 1997). Because Gakkel Ridge represents the lower end member in terms of spreading rate, we expect to find spinels with very fertile, Cr-poor compositions that reflect the lowest degree of melting on the global mid-ocean ridge system. For this reason, we located and studied relict spinel compositions in unusually heavily altered serpentinized mantle peridotites from Gakkel Ridge.

2. Results

The abyssal peridotite fragments were collected in 1987 in box core KAL 11/370-5 during cruise ARK IV/3 of the RV Polarstern at a water depth of 4570 m at 85°54′N, 22°43′E (Thiede, 1988) (Fig. 1). Altered basalt fragments were recovered in the same box core (Mühe et al., 1991, 1993). At this location, the full spreading rate is 1.19 cm/year (Coakley and Cochran, 1998), about half that of the Mid-Atlantic Ridge. The sampling location is on the southern flank of the ridge at a distance of 3.3 km to the central axial valley (Mühe et al., 1991). This corresponds to a crustal age of 500 ka.

About 10 serpentinite fragments with diameters from 5 up to >10 cm (fist size) were studied (one to four polished thin sections per sample). As a result of serpentinization and subsequent ocean floor weathering, no primary silicates were preserved, but textures of pyroxene pseudomorphs and spinels clearly indicate a mantle origin. Cr-spinels of most of the samples appear completely oxidized and opaque in thin section. One sample (KAL 11/370-5-4) contains small relicts of apparently unaltered spinel cores surrounded by alteration products. The spinels are pale yellow-brown in transmitted light indicating a low Cr content as observed in other relatively fertile peridotites. A backscattered electron image (Fig. 2) shows a porphyroclastic spinel from this sample, with a highly irregular holly-leaf shape that is typical for residual mantle rocks. Alteration progresses along fractures in the spinel. Dark grey areas show unaltered, primary Cr-spinel, whereas altered spinel is characterized by fine-grained, bright areas.

Several electron microprobe line profiles were run across the spinels in order to assess the degree of zoning imposed as a result of subsolidus reequilibration or low-temperature alteration. For this purpose, selected elements' intensities (Al, Cr, Mg, and Fe) were measured on a JEOL JXA 8900RL electron probe microanalyzer using an acceleration potential of 20 kV, a beam current of 20 nA, a spot size of 2 μm, an interval of 1 μm and a dwell time of 1 s on each spot. The result of one of these line scans is also shown in Fig. 2. Fresh domains have constant counting rates for all elements that drastically change at fractures and, most importantly, at the weathering front. Within the fresh region, no compositional

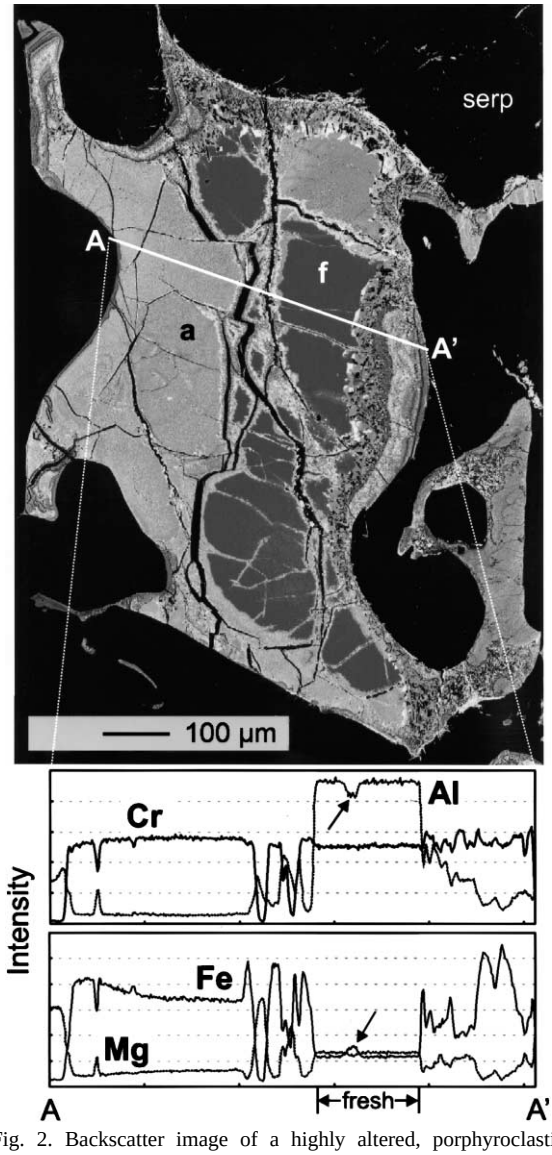

Fig. 2. Backscatter image of a highly altered, porphyroclastic spinel grain from serpentinized peridotite sample KAL 11/370-5-4. Dark grey areas represent unaltered, fresh spinel (f), bright areas are altered zones (a) and serp denotes the serpentinized silicate matrix. Element intensities of Cr, Al, Mg and Fe across profile A–A′ profile are shown below. The unaltered region is highlighted in grey. Note the rapid decrease of Al at the boundary from fresh to altered spinel and the constant Cr intensity in the fresh as well as in the altered zones. The arrows in the grey highlighted area of the element profiles show the effect of a thin fracture that runs subparallel to the profile, resulting in a slight but significant decrease in aluminium and a similar increase in iron content.

zoning is observed. In the altered material, Al is rapidly removed from the spinel lattice and Fe is added so the altered material consists mostly of iron oxides. Cr counting rates remain unchanged in the altered regions (bright) with respect to the fresh spinel. This shows the highly immobile nature of chromium during alteration.

Spot analyses were obtained in the centers of fresh areas of four different spinel porphyroclasts by electron microprobe (20 kV, 20 nA, spot size 2 μm). The average composition for each grain (two or three analyses each) is shown in Table 1. Fresh spinels from sample KAL 11/370-5-4 peridotite have Cr# [molar ratio Cr/(Cr + Al)] between 0.232 and 0.246. Their titanium content is very low (average TiO_2: 0.03%). At the immediate contact to the altered regions, only the Fe^{3+} and Ti contents are slightly higher.

Table 1
Major element compositions (wt.%) of spinels in Gakkel Ridge sample KAL 11/370-5-4
All reported values are averages of three analyses per grain.

	Grain 1	Grain 2	Grain 3	Grain 4
Oxides				
TiO_2	0.05	0.03	0.02	0.04
Al_2O_3	45.68	45.08	46.41	45.89
Cr_2O_3	21.84	21.95	20.86	21.53
FeO	13.20	13.94	13.18	13.53
MgO	19.00	18.53	18.82	18.72
MnO	0.14	0.18	0.17	0.18
CaO	0.00	0.01	0.01	0.01
NiO	0.25	0.22	0.24	0.26
Na_2O	0.00	0.01	0.02	0.00
K_2O	0.00	0.00	0.01	0.00
Sum	100.18	99.95	99.74	100.15
Cations (32 oxygens per formula unit)				
Ti	0.01	0.00	0.00	0.01
Al	11.66	11.58	11.86	11.72
Cr	3.74	3.78	3.58	3.69
Fe_t	2.39	2.54	2.39	2.45
Mg	6.13	6.02	6.08	6.05
Mn	0.03	0.03	0.03	0.03
Ca	0.00	0.00	0.00	0.00
Ni	0.04	0.04	0.04	0.04
Na	0.00	0.00	0.01	0.00
K	0.00	0.00	0.00	0.00
Sum	24	24	24	24
Fe^{3+}	0.59	0.64	0.56	0.57
Cr/(Cr + Al)	0.243	0.246	0.232	0.239
$Mg/(Mg + Fe^{2+})$	0.772	0.759	0.769	0.763

The microprobe profiles and spot analyses show that the transition from the fresh spinel (yellow-brown in transmitted light) into oxidized (opaque) material is a sharp contact that is characterized by dramatic differences in Al and Fe. In the fresh domains, the composition remains constant, except for the direct vicinity ($\sim < 5$ μm) of cracks. At these fractures, excursions in aluminium and iron content (arrows in Fig. 2) are highly visible in BSE image and microprobe profiles. These features indicate that alteration has proceeded along an alteration front outward from cracks in the spinel and has not affected their cores. The analyses listed in Table 1 thus reflect the primary spinel composition.

3. Discussion

The Cr# and Mg# (molar ratio $Mg/(Mg + Fe^{2+})$) of spinel has proven to be a very sensitive indicator for melt extraction (Dick, 1989; Dick and Bullen, 1984; Dick et al., 1984; Johnson and Dick, 1992; Johnson et al., 1990; Michael and Bonatti, 1985), melt–peridotite reactions during focused porous flow (Allan and Dick, 1996; Dick and Natland, 1996; Kelemen et al., 1992, 1997) and melt–wall rock reactions in the vicinity of intruding magmatic veins (Cannat et al., 1997; Hellebrand et al., 1999). With increasing degree of melting, decreasing activity of aluminium in the peridotite leads to an increase in equilibrium Cr# in spinel as shown in the melting trend of Fig. 3 (Hellebrand et al., 2001).

Also shown in Fig. 3 are spinel compositions from other selected localities, illustrating the limited local variation in residual mantle rocks. A systematic study of residual peridotites in the MARK area (Mid-Atlantic Ridge near Kane Fracture Zone at 24°N) has shown very limited local variation of spinel compositions (Fig. 3). On a regional scale, however, the mantle rocks become increasingly depleted away from the Kane Fracture Zone (Ghose et al., 1996). The samples from these dredge hauls and boreholes were specifically selected because they do not contain plagioclase (Seyler and Bonatti, 1997) or crosscutting magmatic veins (Hellebrand et al., 1999; Niida, 1997), which may significantly modify the host rock composition and produce large compositional variations, even on thin section scale. There-

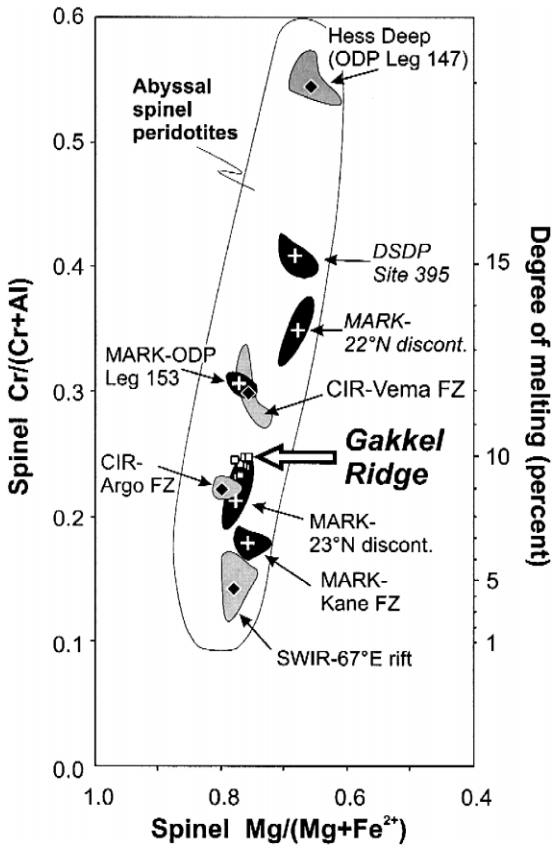

Fig. 3. Spinel Cr# vs. Mg# of serpentinized peridotite sample KAL 11/370-5-4. All point analyses are shown. Spinel compositions from other abyssal peridotites are shown for comparison to illustrate the fairly narrow compositional range of plagioclase-free and vein-free peridotites from one location. Closed diamonds are the average of each range represented by the enclosing fields. The studied Gakkel Ridge peridotite is significantly more depleted than the most fertile spinel peridotite from the faster spreading easternmost SWIR. MARK area peridotites (pluses) (Ghose et al., 1996) illustrate regional variations, possibly as a result of the cooling effect of the Kane FZ. Spinel peridotite field is after Dick and Bullen (1984), other data after Hellebrand et al. (submitted for publication).

fore, it is important to estimate whether plagioclase was initially present in the peridotite. Plagioclase in abyssal peridotites is commonly interpreted as a trapped melt product in the widest sense (Dick, 1989), rather than being formed during the transition from spinel to plagioclase stability field (Hamlyn and Bonatti, 1980). Plagioclase-bearing peridotites commonly have high (>0.1 wt.%) TiO_2 contents (Dick, 1989; Dick and Bullen, 1984) as shown in Fig. 4. The very low Ti content in the spinel of Gakkel Ridge sample supports the absence of plagioclase and attests to the residual nature of this particular sample.

The composition of basaltic glass shards recovered along with these peridotites indicates some of the lowest degrees of melting ever observed along the mid-ocean ridges. The not particularly low Cr# of the peridotites is nowhere near the extremes observed at mid-ocean ridges. Indeed, many spinels from residual harzburgites from the Southwest Indian Ridge and American–Antarctic Ridge (AAR) (Dick, 1989) have lower Cr#. In fact, the Cr# of these Gakkel Ridge samples corresponds to an estimated degree of fractional melting of 9% (Hellebrand et al., 2001). This is at least 5% more than the most fertile SWIR and AAR peridotites, which have spinel Cr# of 0.10–0.15.

In order to test for the presence or absence of a spreading rate dependence of abyssal peridotite spinel compositions, Gakkel Ridge peridotites should be compared to other abyssal peridotites from similar non-transform settings. As seen in the MARK area peridotites, the transform fault effect strongly influences peridotite compositions. At Kane FZ, fertile peridotites with an average spinel Cr# of 0.17 occur, a value that systematically increases to a maximum of 0.41 away from the transform (Fig. 3) (Ghose et al., 1996). This means that the corresponding degree of melting increases from 5% at Kane FZ to 15% near the center of the segment (Hellebrand et al., 2001). Because of its magnitude, the transform fault effect, which is superimposed on the spreading rate effect, produces a strong bias in the global geodynamic systematics from a residual mantle perspective since most abyssal peridotites were collected directly at fracture zone walls. Large-offset transform faults are omnipresent along the very slow spreading SWIR. By this reasoning, the fertility of most SWIR peridotites is the result of the slow spreading rate combined with the cooling effect of the transform faults.

At Gakkel Ridge, spreading is orthogonal and transform faults appear to be absent (Coakley and Cochran, 1998). In order to address the effect of the spreading rate, the spinels from these partial-melting residues should be compared to similar axial peridotite occurrences. Although they are not as common

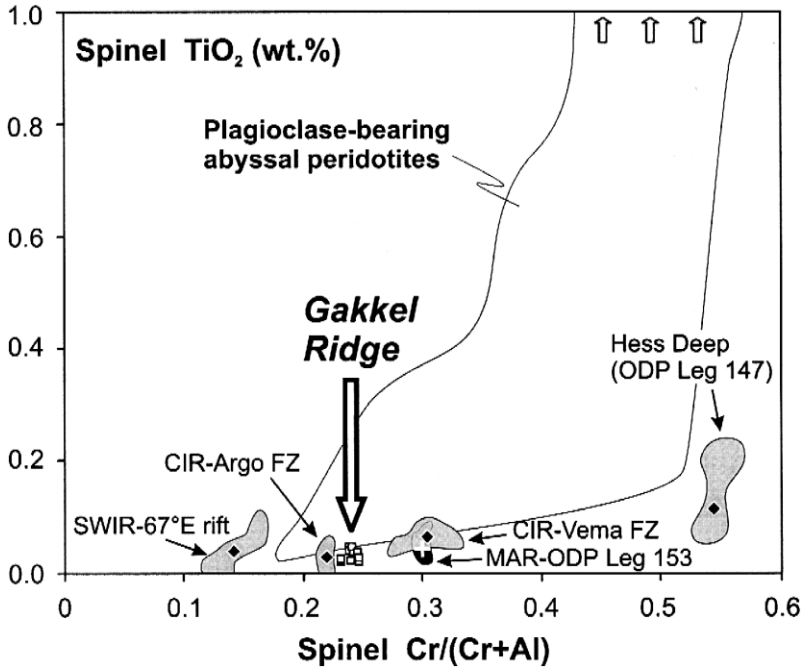

Fig. 4. Spinel TiO_2 vs. Cr# content of serpentinized peridotite sample KAL 11/370-5-4. All point analyses are shown. Spinels from plagioclase-free peridotites are characterized by very low Ti contents, whereas plagioclase-bearing peridotite have elevated titanium concentrations, often exceeding 1 wt.%. Most plagioclase-bearing peridotites have higher Cr# than residual mantle rocks. Plagioclase–peridotite compositions are from Dick and Bullen (1984), Dick et al. (1984) and own unpublished results.

as in fracture zones, such peridotites do occur (Cannat, 1993; Cannat et al., 1995), but published mineral data are scarce. Only for Hess Deep in the Pacific (Dick and Natland, 1996) and the MARK area (Ghose et al., 1996; Niida, 1997; Sinton, 1978) are published spinel data available. Further, we have unpublished data for Green Rock Hill on the southernmost Central Indian Ridge (CIR), the easternmost SWIR rift, and the CIR axis at 12°S (Hellebrand et al., submitted for publication). In Fig. 5A, spinel Cr# of these non-transform peridotites are plotted vs. the local spreading rate (DeMets et al., 1990). Despite the scarcity of the data, spinel Cr# clearly increases with spreading rate.

We can now apply a quantitative melting tool that uses spinel compositions from residual peridotites to estimate global variations in crustal thickness, and its dependence on spreading rate. The observed relationship between cpx trace element composition and spinel Cr# yields the empirical fractional melting function, as proposed by (Hellebrand et al., 2001)

$$F_{sp} = 0.1\ln(\mathrm{Cr\#}) + 0.24. \quad (1)$$

In principle, peridotite compositions provide a direct estimate of the maximum degree of melting of the melting column. Under passive upwelling conditions, the total extent of melting, F_{max}, can be expressed as:

$$F_{max} = B(Z_0 - Z_f), \quad (2)$$

where B is the melt production rate (%/km) and Z_0 and Z_f are the initial- and final depth of melting, respectively (Forsyth, 1993). Further, the crustal thickness, H, can also be expressed as a function of these variables:

$$H = \frac{B(Z_0^2 - Z_f^2)}{2}. \quad (3)$$

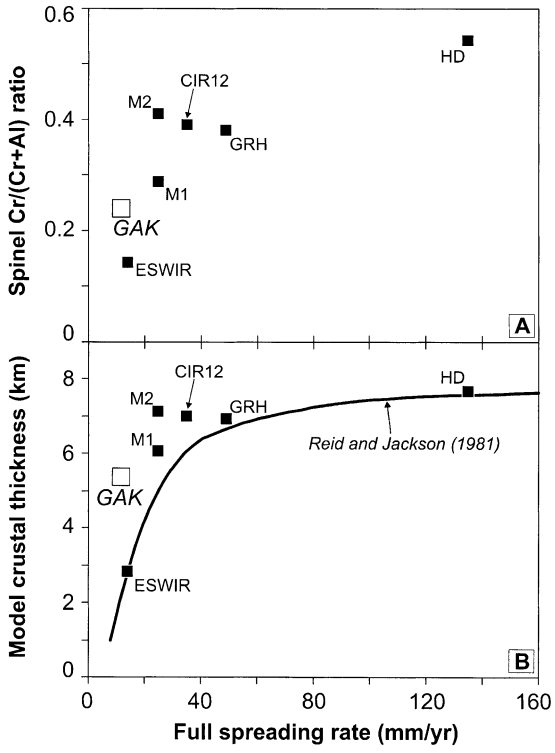

Fig. 5. (A) Local full spreading rate vs. spinel Cr# of non-transform peridotites, and (B) model crustal thickness. Crustal thickness is calculated from average local spinel compositions, applying the empirical melting model of Hellebrand et al. (2001) and equations by Forsyth (1993). Thick black curve represents predicted spreading-rate dependent crustal thickness favored by Reid and Jackson (1981). Spreading rates (full) are calculated from Nuvel 1 using the online calculator at InterRidge homepage. Location codes are listed in Table 2.

Assuming that melt production rate B is constant throughout the melting column, and melting commences at a constant depth of 70 km, the crustal thickness H can be directly calculated from $F_{max} = F_{sp}$:

$$H = Z_0 F - \frac{F^2}{2B}. \quad (4)$$

For the Gakkel Ridge spinels, a Cr# of 0.24 corresponds to 9.7% of melting, which yields a 5.4-km thick crust. The results for other non-transform abyssal peridotites are summarized in Table 2. In Fig. 5B, the calculated crustal thickness for each average non-transform peridotite occurrence is plotted vs. spreading rate. The thick black curve is a predicted relationship between spreading rate and oceanic crustal thickness, which is relatively constant at fast spreading rates, but is believed to decrease rapidly at very slow spreading rates (Reid and Jackson, 1981). Clearly, Gakkel Ridge sample yields a model crustal thickness that is much thicker than expected from this model. The thin crust at Gakkel Ridge, predicted by the thermal model of Reid and Jackson agrees well with the observed crustal thickness estimated from gravity data at Gakkel Ridge (Coakley and Cochran, 1998). There are three possible explanations to explain why Gakkel Ridge peridotite produces this unexpected result.

The first interpretation is that the regional degree of melting is not as low as predicted from global correlation estimates. This would imply that mantle melting in general is not as strongly controlled by spreading rate as by other factors such as mantle temperature, mantle source composition or ridge obliquity. This interpretation, however, is not in agreement with the basalt compositions that indicate an extremely low degree of melting.

Table 2
Locations and characteristics of non-transform residual spinel peridotites

Location	Dredge/drillhole	Latitude (N/S)	Longitude (E/W)	Spreading rate (mm/year)	Spinel Cr#	Degree of melting[a]	Crustal thickness	Code in Fig. 5
Hess Deep (EPR)	ODP Site 895	2°17′N	101°27′W	135	0.54	17.9	7.7	HD
Green Rock Hill (CIR)	SO92/74GTV	25°24′S	69°46′E	49	0.38	14.3	6.9	GRH
CIR 12°S	CIRCE93	12°25′S	65°56′E	35	0.39	14.6	7.0	CIR12
MARK area	ODP Site 920	23°20′N	45°01′W	25	0.29	11.6	6.1	M1
MARK area	DSDP Site 395	22°45′N	46°05′W	25	0.41	15.1	7.1	M2
Easternmost SWIR	AII 93: 5-9	26°30′S	67°27′E	14	0.14	4.5	2.8	ESWIR
Gakkel Ridge	KAL 11/370-5	85°54′N	22°43′E	12	0.24	9.7	5.4	GAK

[a] Hellebrand et al. (2001).

A second possibility is that the studied sample does not represent the local/dredge average, but may be an outlying point due to natural heterogeneity. Significant modal and compositional variations of peridotites within a single dredge haul or location are common (Dick and Bullen, 1984; Dick et al., 1984; Dick, 1989). However, the largest variations are mostly found in areas with abundant plagioclase-bearing peridotites, which are non-residual rocks (Dick, 1989; Seyler and Bonatti, 1997). Plagioclase-free peridotites from a single drill hole, away from crosscutting magmatic dikelets, have a fairly narrow Cr# range, typically ~0.02–0.06 (Dick and Natland, 1996; Niida, 1997; Sinton, 1978), as do most dredged residual abyssal peridotites. However, exceptions to this general rule exist, such as peridotites from Marie Celeste FZ on the CIR (Cr# from 0.17 to 0.29 within a single dredge) and an outcrop on the CIR axis at 12°S (Cr# from 0.31 to 0.53 within a single dredge) (Hellebrand et al., submitted for publication). Accepting that these values represent the extreme local variations at a scale sampled by dredging, we can assume that the underlying average Cr# of the mantle at this part of Gakkel Ridge is not dramatically different from what we have measured.

Finally, these spinel compositions might reflect the heterogeneity of melt extraction at ultraslow spreading ridges. At slow spreading ridges, the degree of melting from the mantle has been proposed to vary along the spreading center (Whitehead et al., 1984). More melt is extracted at the center of the segment and less at the distal ends. The melt is laterally focused towards the centers of segments, as suggested by gravity patterns (Lin et al., 1990). This effect is expected to be more pronounced at ultraslow spreading rates, though insufficient data currently exist to test this proposition. The intermediate spinel compositions seen here might then represent the center of a spreading cell. This would be consistent with their association with basalts. The lower average degree of melting of the basalts (Mühe et al., 1991, 1993, 1997) would agree with this scenario, as the basalts average a much larger melting volume than is sampled by the peridotites. Despite the scant evidence available regarding magmatic segmentation along Gakkel Ridge (Coakley and Cochran, 1998), this remains the most plausible scenario.

4. Conclusions

(1) Spinel cores in this study represent primary mantle values despite advanced serpentinization and oxidation of the rock.

(2) Overall degrees of melting are relatively low compared to global abyssal peridotites.

(3) The extremely low degree of melting observed in spatially associated basalt glasses (Mühe et al., 1991, 1993, 1997) is not seen in these samples. Many areas (mostly on the very slow spreading SW Indian Ridge) show equivalent or lower Cr#.

(4) Model crustal thickness at the ultraslow spreading Gakkel Ridge, as calculated from the peridotite spinel composition, is thicker than estimated from existing gravity data and predicted spreading-rate dependent correlations.

(5) The reason for this greater than expected depletion may be local heterogeneity due to enhanced melt focussing at an ultraslow spreading ridge.

These spinel analyses from a single sample of mid-ocean ridge mantle represent just a beginning. They are not in themselves sufficient to characterize an entire mid-ocean ridge. Further sampling and analysis of Arctic mantle rocks are required to fully address the evolution of this unique mid-ocean ridge system.

Acknowledgements

Fig. 1 was generated using the GMT online map creation at http://www.aquarius.geomar.de. We thank Kevin Johnson and Honique Seyler for their constructive reviews.

References

Allan, J.F., Dick, H.J.B., 1996. Cr-rich spinel as a tracer for melt migration and melt–wall rock interaction in the mantle: Hess Deep, Leg 147. Proc. Ocean Drill. Program: Sci. Results 147, 157–172.

Cannat, M., 1993. Emplacement of mantle rocks in the seafloor at mid-ocean ridges. J. Geophys. Res. 98, 4163–4172.

Cannat, M. et al., 1995. Thin crust, ultramafic exposures, and rugged faulting patterns at the Mid-Atlantic Ridge (22°–24°N). Geology 23, 49–52.

Cannat, M., Chatin, F., Whitechurch, H., Ceuleneer, G., 1997. Gabbroic rocks trapped in the upper mantle at the Mid-Atlantic Ridge. Proc. Ocean Drill. Program: Sci. Results 153, 243–264.

Coakley, B.J., Cochran, J.R., 1998. Gravity evidence of very thin crust at the Gakkel Ridge (Arctic Ocean). Earth Planet. Sci. Lett. 162, 81–95.

DeMets, C., Gordon, R.G., Argus, D.F., Stein, S., 1990. Current plate motions. Geophys. J. Int. 101, 425–478.

Dick, H.J.B., 1989. Abyssal peridotites, very slow spreading ridges and ocean ridge magmatism. Geol. Soc. London, Spec. Publ. 42, 71–105.

Dick, H.J.B., Bullen, T., 1984. Chromian spinel as a petrogenetic indicator in abyssal and alpine-type peridotites and spatially associated lavas. Contrib. Mineral. Petrol. 86, 54–76.

Dick, H.J.B., Natland, J.H., 1996. Late-stage melt evolution and transport in the shallow mantle beneath the East Pacific Rise. Proc. Ocean Drill. Program: Sci. Results 147, 103–134.

Dick, H.J.B., Fisher, R.L., Bryan, W.B., 1984. Mineralogic variability of the uppermost mantle along mid-ocean ridges. Earth Planet. Sci. Lett. 69, 88–106.

Forsyth, D.W., 1993. Crustal thickness and the average depth and degree of melting in fractional melting models of passive flow beneath mid-ocean ridges. J. Geophys. Res. 98, 16073–16079.

Ghose, I., Cannat, M., Seyler, M., 1996. Transform fault effect on mantle melting in the MARK area (Mid-Atlantic Ridge south of the Kane transform). Geology 24, 1139–1142.

Hamlyn, P.R., Bonatti, E., 1980. Petrology of mantle-derived ultramafics from the Owen Fracture Zone, Northwest Indian Ocean: implications for the nature of the oceanic upper mantle. Earth Planet. Sci. Lett. 48, 65–79.

Hellebrand, E.W., Snow, J.E., Dick, H.J.B., Devey, C.W., Hofmann, A.W., 1999. Reactive crack flow in the oceanic mantle: an ion probe study on cpx from vein-bearing abyssal peridotites. Ofioliti 24, 106–107.

Hellebrand, E., Snow, J.E., Dick, H.J.B., Hofmann, A.W., 2001. Coupled major and trace elements as indicators of the extent of melting in mid-ocean-ridge peridotites. Nature 410, 677–681.

Hellebrand, E., Snow, J.E., Hofmann, A.W. Garnet-field melting and late-stage refertilization in 'residual' abyssal peridotites from the Central Indian Ridge. J. Petrol., submitted for publication.

Johnson, K.T.M., Dick, H.J.B., 1992. Open system melting and temporal and spatial variation of peridotite and basalt at the Atlantis II fracture zone. J. Geophys. Res. 97, 9219–9241.

Johnson, K.T.M., Dick, H.J.B., Shimizu, N., 1990. Melting in the oceanic upper mantle; an ion microprobe study of diopsides in abyssal peridotites. J. Geophys. Res. 95, 2661–2678.

Kelemen, P.B., Dick, H.J.B., Quick, J.E., 1992. Formation of harzburgite by pervasive melt/rock reaction in the upper mantle. Nature 358, 635–641.

Kelemen, P.B., Hirth, G., Shimizu, N., Spiegelman, M., Dick, H.J.B., 1997. A review of melt migration processes in the adiabatically upwelling mantle beneath oceanic spreading ridges. Philos. Trans. R. Soc. London 355, 283–318.

Klein, E.M., Langmuir, C.H., 1987. Global correlations of ocean ridge basalts with axial depth and crustal thickness. J. Geophys. Res. 92, 8089–8115.

Langmuir, C.H., Klein, E.M., Plank, T., 1992. Petrologic systematics of mid-ocean ridge basalts: constraints on melt generation beneath ocean ridges. In: Phipps-Morgan, J., Blackman, D.K., Sinton, J.M. (Eds.), Mantle Flow and Melt Generation at Mid-Ocean Ridges. AGU Monograph, pp. 183–280.

Lin, J., Purdy, G.M., Schouten, H., Sempere, J.C., Zervas, C., 1990. Evidence from gravity data for focused magmatic accretion along the Mid-Atlantic Ridge. Nature 344, 627–632.

Michael, P.J., Bonatti, E., 1985. Peridotite composition from the North Atlantic; regional and tectonic variations and implications for partial melting. Earth Planet. Sci. Lett. 73, 91–104.

Mühe, R., Bohrmann, H., Hörmann, P.K., Thiede, J., Stoffers, P., 1991. Spinifex basalts with komatiite–tholeiite trend from the Nansen–Gakkel Ridge (Arctic Ocean). Tectonophysics 190, 95–108.

Mühe, R., Devey, C.W., Bohrmann, H., 1993. Isotope and trace element geochemistry of MORB from the Nansen–Gakkel Ridge at 86° North. Earth Planet. Sci. Lett. 120, 103–109.

Mühe, R., Bohrmann, H., Garbe-Schönberg, D., Kassens, H., 1997. E-MORB glasses from the Gakkel Ridge (Arctic Ocean) at 87°N: evidence for the Earth's most northerly volcanic activity. Earth Planet. Sci. Lett. 152, 1–9.

Niida, K., 1997. Mineralogy of MARK peridotites: replacement through magma channeling examined from Hole 920D, MARK area. Proc. Ocean Drill. Program: Sci. Results 153, 243–264.

Niu, Y., Hekinian, R., 1997. Spreading-rate dependence of the extent of mantle melting beneath ocean ridges. Nature 385, 326–329.

Reid, I., Jackson, R., 1981. Oceanic spreading rate and crustal thickness. Mar. Geophys. Res. 5, 165–172.

Seyler, M., Bonatti, E., 1997. Regional-scale melt–rock interaction in lherzolitic mantle in the Romanche fracture zone (Atlantic Ocean). Earth Planet. Sci. Lett. 146, 273–287.

Sinton, J., 1978. Petrology of (alpine-type) peridotites from Site 395, DSDP Leg 45. Initial Rep. Deep Sea Drill. Proj. 45, 595–601.

Thiede, J., 1988. Scientific cruise report of Arctic Expedition ARK IV/3. Ber. Polarforschung, Rep. Polar Res. 43, 236 pp.

Whitehead, J.A., Dick, H.J.B., Schouten, H., 1984. A mechanism for magmatic accretion under spreading ridges. Nature 312, 146–148.